

RESURRECTION OF THE BOHR/SOMMERFELD
THEORY OF ATOMIC STRUCTURE
[4]
THE ADDITION OF
SMALL RELATIVISTIC CORRECTION TERMS
INCORPORATING THE LAMB SHIFT.

Peter G.Bass.

ABSTRACT.

The Bohr/Sommerfeld theory of atomic structure, as so far re-stated in [7], [8] and [9], is herein further developed to incorporate small relativistic energy correction terms that lead to the Lamb Shift. These terms are shown to be due to primarily two causes, (i) the distributed nature of electron charge, and (ii) the dynamic distance of the nucleus from the central point of orbital rotation. The first of these, (i), is augmented by consideration of the nature of the electron spin matter wave radius.

1 Introduction.

The Lamb Shift is a very small difference in the orbital energies of the s and p(-) orbitals, primarily in the 2nd shell although it is also apparent down to at least shell 8. In the modern quantum mechanics/quantum electrodynamics theory of atomic structure, the Lamb Shift is attributed to changes in the electron self energy resulting from its interaction with fluctuating electric and magnetic fields that contribute to the zero point energy of the vacuum. Thereby the purported potentiality of the electron to emit and re-absorb virtual photons, which contribute to electron self energy, result in the value of this parameter being different in different orbitals, [1], [2], [3], [4].

In the resurrected Bohr/Sommerfeld theory presented here, because the electron is treated as a real physical particle, albeit with a dual corpuscular/matter wave existence, recourse to quantum electrodynamic phenomena such as described above, to explain the Lamb Shift, is not necessary as other simpler physical causes become apparent.

In this resurrected theory, the development to date has treated both the nucleus and, more particularly, the electron as spinning point charges. When the electron is afforded finite dimensions, in order that it subsequently conforms to the spin angular momentum criteria, especially in circular orbits, it will be proposed that its spin matter wave radius must become a variable that is to be determined. When this is coupled with the introduction of the concept that the electron charge is distributed uniformly on its outer surface, a small additional energy term is created, of relativistic magnitude, that must be added to the fine structure orbital energy levels.

In addition to the above, the development to date, while incorporating the finite mass of the nucleus, has only partly taken account of the fact that due to this finite mass, it, together with the electron, will orbit about a central point of rotation. The ratio of the distance of the nucleus from this central point of rotation, to that of the electron, will be the inverse of the ratio of their

masses. Augmenting this is the fact that, as shown in [9], the spin - orbit magnetic dipole coupled precession rate of the nucleus is significantly greater than that of the electron. When allowance for these latter factors is introduced, a further small additional energy term of relativistic magnitude results that is also to be added to the fine structure orbital energy levels.

When these extra terms are introduced the overall orbital energy levels are seen to incorporate the Lamb Shift. The resulting energy levels and emission spectra so obtained can then be compared in detail with those in [5], which is believed to be the most accurate published data on outer shell single electron atoms.

Note that in the mathematical derivations in this paper, a parameter will only be defined if it has not previously been so in earlier papers in this series, i.e. [6], [7], [8] and [9].

2 The Energy Correction Term Source Components.

2.1 Derivation of the Central Coulomb Force Taking Into Account the Distributed Nature of the Spinning Electron Charge.

In this derivation it is to be noted that because of the high spin rate of the electron at the point of orbital transition, account must be taken of the Lorentz - Fitzgerald contraction of circumferential dimensions.

The derivation here will be restricted to the electron, similar effects generated by the nucleus are discussed in Section 2.4.

Consider Fig. 2.1 below as representative of a spinning electron in any orbital.

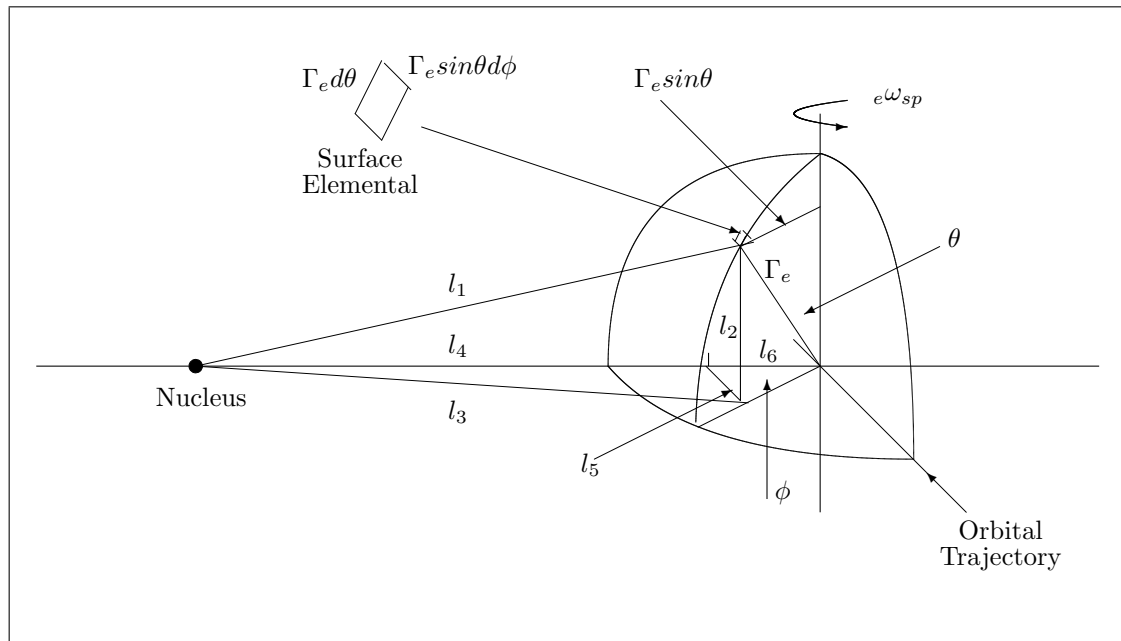


Fig. 2.1 - The Spinning Electron.

The charge on the nucleus is $+Ze$.

The surface charge density on the electron is $-\Delta e$.

The distance between the centre of the two particles is r .

The area of the electron elemental at rest is

$$\Delta\Lambda = \Gamma_e^2 \sin\theta d\theta d\phi \quad (2.1)$$

Where

Λ is the surface area of the electron

Γ_e is the matter wave radius of the electron, (strictly this parameter only applies when the electron is rotating, but for the purpose of this analysis can be introduced at this point).

and all other parameters are as shown in Fig 2.1.

With the electron shell spinning at the high angular rate of ${}_{e}\omega_{sp}$ as shown, all circumferential dimensions will be subject to Lorentz-Fitzgerald contraction. Thus the surface area of the electron elemental, becomes

$$\Delta\Lambda^* = \Gamma_e^2 \sin\theta \left(1 - \frac{{}_{e}\omega_{sp}^2 \Gamma_e^2 \sin^2\theta}{c^2}\right)^{1/2} d\theta d\phi \quad (2.2)$$

Where

c is the velocity of light.

In [8] it was proposed that electron orbit shell transitions took place via the emission of a photon because the surface velocity of the circumference of the spinning electron tended to exceed the terminal velocity, (\sim the velocity of light), in the Relativistic Domain D_0 , (Pseudo-Euclidean Space-Time), (see [10] for an explanation of this). Thus in (2.2) above, at the point of an orbit shell transition

$${}_{e}\omega_{sp}\Gamma_e = c \quad (2.3)$$

so that (2.2) becomes

$$\Delta\Lambda^* = \Gamma_e^2 \sin\theta \cos\theta d\theta d\phi \quad (2.4)$$

Therefore the coulomb coupling energy between the nucleus and the electron elemental is

$$\Delta E_{coul} = -\frac{Ze\Delta e\Gamma_e^2 \sin\theta \cos\theta d\theta d\phi}{l_1} \quad (2.5)$$

It is now necessary to determine the distance l_1 which must also take account of Lorentz-Fitzgerald contraction of circumferential dimensions associated with the electron. From Fig. 2.1

$$l_1 = (l_3^2 + l_2^2)^{1/2} \quad (2.6)$$

Where

$$l_2 = \Gamma_e \cos\theta \quad (2.7)$$

In (2.6)

$$l_3 = (l_4^2 + l_5^2)^{1/2} \quad (2.8)$$

and

$$l_4 = r - l_6 \quad (2.9)$$

Where

r is the distance between the centre of the two particles.

Then

$$l_5 = \Gamma_e \sin \theta \cos \theta \cos \phi \quad (2.10)$$

and

$$l_6 = \Gamma_e \sin \theta \cos \theta \sin \phi \quad (2.11)$$

In these last two equations, (2.10) and (2.11), the effects of Lorentz-Fitzgerald contraction of circumferential dimensions have been incorporated. Details of this are shown in Appendix C. Substitution of (2.9), (2.10) and (2.11) into (2.8) gives

$$l_3 = \left\{ (r - \Gamma_e \sin \theta \cos \theta \cos \phi)^2 + \Gamma_e^2 \sin^2 \theta \cos^2 \theta \sin^2 \phi \right\}^{1/2} \quad (2.12)$$

Which reduces to

$$l_3 = (r^2 - 2r\Gamma_e \sin \theta \cos \theta \cos \phi + \Gamma_e^2 \sin^2 \theta \cos^2 \theta)^{1/2} \quad (2.13)$$

Substitution of (2.13) and (2.7) into (2.6) then gives

$$l_1 = (r^2 - 2r\Gamma_e \sin \theta \cos \theta \cos \phi + \Gamma_e^2 \sin^2 \theta \cos^2 \theta + \Gamma_e^2 \cos^2 \theta)^{1/2} \quad (2.14)$$

Which in turn reduces to

$$l_1 = r \left(1 + \frac{\Gamma_e^2}{r^2} - 2\frac{\Gamma_e}{r} \sin \theta \cos \theta \cos \phi - \frac{\Gamma_e^2}{r^2} \sin^4 \theta \right)^{1/2} \quad (2.15)$$

So that in (2.5) this gives for the elemental coupling energy

$$\Delta E_{coul} = - \frac{Ze\Delta e\Gamma_e^2 \sin \theta \cos \theta d\theta d\phi}{r \left(1 + \frac{\Gamma_e^2}{r^2} - 2\frac{\Gamma_e}{r} \sin \theta \cos \theta \cos \phi - \frac{\Gamma_e^2}{r^2} \sin^4 \theta \right)^{1/2}} \quad (2.16)$$

In (2.16), because $r \gg \Gamma_e$, the denominator can be binomially expanded retaining only terms up to $1/r^3$. This then yields

$$\Delta E_{coul} = - \frac{Ze\Delta e\Gamma_e^2 \sin \theta \cos \theta}{r} \left(1 - \frac{\Gamma_e^2}{2r^2} + \frac{\Gamma_e}{r} \sin \theta \cos \theta \cos \phi + \frac{\Gamma_e^2}{2r^2} \sin^4 \theta + \frac{3\Gamma_e^2}{2r^2} \sin^2 \theta \cos^2 \theta \cos^2 \phi \right) d\theta d\phi \quad (2.17)$$

Integrating over the complete electron spherical shell

$$E_{coul} = -\frac{2Ze\Delta e\Gamma_e^2}{r} \int_{\phi=0}^{2\pi} \int_{\theta=0}^{\pi/2} \left(\begin{array}{l} \left(1 - \frac{\Gamma_e^2}{2r^2}\right) \sin \theta \cos \theta + \frac{\Gamma_e}{r} \sin^2 \theta \cos^2 \theta \cos \phi + \\ \frac{\Gamma_e^2}{2r^2} \sin^5 \theta \cos \theta + \frac{3\Gamma_e^2}{2r^2} \sin^3 \theta \cos^3 \theta \cos^2 \phi \end{array} \right) d\theta d\phi \quad (2.18)$$

Where in the integral with respect to θ , advantage of symmetry has been taken to simplify the integration process. The integral with respect to ϕ is simple and is taken first to yield

$$E_{coul} = -\frac{4\pi Ze\Delta e\Gamma_e^2}{r} \int_{\theta=0}^{\pi/2} \left\{ \begin{array}{l} \left(1 - \frac{\Gamma_e^2}{2r^2}\right) \sin \theta \cos \theta + \frac{\Gamma_e^2}{2r^2} \sin^5 \theta \cos \theta + \\ \frac{3\Gamma_e^2}{4r^2} \sin^3 \theta \cos^3 \theta \end{array} \right\} d\theta \quad (2.19)$$

In Appendix B it is shown that the surface area of a sphere, spinning such that its circumferential velocity tends to the velocity of light is exactly half that when at rest. Incorporating this into (2.19) yields

$$E_{coul} = -\frac{2Ze^2}{r} \int_{\theta=0}^{\pi/2} \left\{ \begin{array}{l} \left(1 - \frac{\Gamma_e^2}{2r^2}\right) \sin \theta \cos \theta + \frac{\Gamma_e^2}{2r^2} \sin^5 \theta \cos \theta + \\ \frac{3\Gamma_e^2}{4r^2} \sin^3 \theta \cos^3 \theta \end{array} \right\} d\theta \quad (2.20)$$

Evaluation of this final integral gives

$$E_{coul} = -\frac{Ze^2}{r} \left(1 - \frac{5\Gamma_e^2}{24r^2}\right) \quad (2.21)$$

This relationship will be further embellished in the next Section via the derivation of the parameter r .

2.2 Derivation of the Effect of the Dynamic Distance of the Nucleus From the Centre of Orbital Motion.

It was shown in [9] that due to the manner in which spin-orbit coupling energy was distributed, the precession rate of the nucleus about the central point of orbital rotation would be considerably greater than that of the electron. The geometry is shown in Fig. 2.2 below.

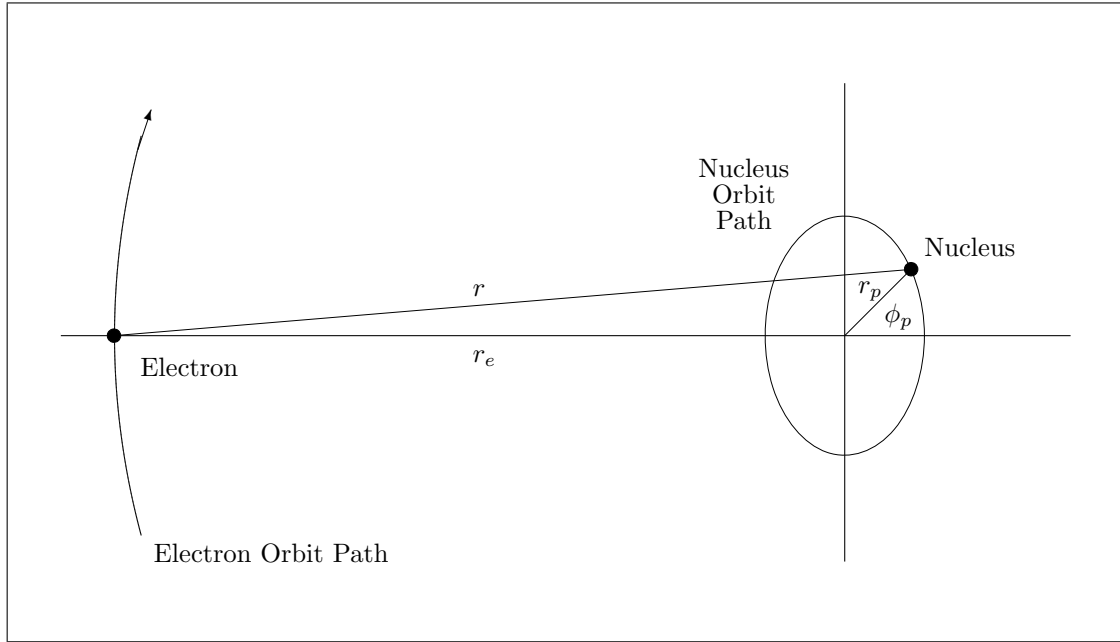


Fig . 2.2 - Electron/Nucleus Orbit Geometry.

By the cosine rule

$$r^2 = r_e^2 + r_p^2 - 2r_e r_p \cos(\pi - \phi_p) \quad (2.22)$$

Which reduces to

$$r^2 = r_e^2 + r_p^2 + 2r_e r_p \cos \phi_p \quad (2.23)$$

In view of the increased angular rate of the orbit of the nucleus, with the electron frozen in the position shown in Fig. 2.2, Eq.(2.23) can be restated as

$$r^2 = r_e^2 + r_p^2 + 2r_e r_p \cos \omega_p t \quad (2.24)$$

Where

ω_p is the angular rate of the proton nucleus.

To determine the effect of this dynamic distance between the two particles, the average of (2.24) around the proton orbital is taken thus

$$\langle r \rangle = r_e \frac{\omega_p}{2\pi} \int_0^{2\pi/\omega_p} \left(1 + \frac{r_p^2}{r_e^2} + 2 \frac{r_p}{r_e} \cos(\omega_p t) \right)^{1/2} dt \quad (2.25)$$

Expanding the square root binomially, ($r_e \gg r_p$), and retaining terms only up to $1/r_e^2$ gives

$$\langle r \rangle = r_e \frac{\omega_p}{2\pi} \int_0^{2\pi/\omega_p} \left(1 + \frac{r_p^2}{2r_e^2} + \frac{r_p}{r_e} \cos(\omega_p t) - \frac{r_p^2}{2r_e^2} \cos^2(\omega_p t) \right) dt \quad (2.26)$$

and this evaluates to

$$\langle r \rangle = r_e \left(1 + \frac{r_p^2}{4r_e^2} \right) \quad (2.27)$$

Inserting this into (2.21) gives for the central coulomb force coupling energy

$$\langle E_{coul} \rangle = -\frac{Ze^2}{r_e \left(1 + \frac{r_p^2}{4r_e^2} \right)} \left\{ 1 - \frac{5\Gamma_e^2}{24r_e^2 \left(1 + \frac{r_p^2}{4r_e^2} \right)^2} \right\} \quad (2.28)$$

Expressing this as

$$\langle E_{coul} \rangle = -\frac{Ze^2}{r_e} \left\{ \left(1 + \frac{r_p^2}{4r_e^2} \right)^{-1} - \frac{5\Gamma_e^2}{24r_e^2} \left(1 + \frac{r_p^2}{4r_e^2} \right)^{-3} \right\} \quad (2.29)$$

Again because $r_e \gg r_p$ both terms inside the main bracket can be binomially expanded retaining only terms up to $1/r_e^2$ thus

$$\langle E_{coul} \rangle = -\frac{Ze^2}{r_e} \left(1 - \frac{r_p^2}{4r_e^2} - \frac{5\Gamma_e^2}{24r_e^2} \right) \quad (2.30)$$

Removing the main central force term from (2.30) leaves the correction terms only thus

$$\langle E_{corr} \rangle = \frac{Ze^2}{r_e^3} \left(\frac{r_p^2}{4} + \frac{5\Gamma_e^2}{24} \right) \quad (2.31)$$

In Section 3.0 this expression will be converted to a form suitable for numerical computation of values, and therefore also suitable for addition to [9], Eq. (3.39), to produce the complete expression for orbital energy of the fine structure. Prior to that, Γ_e must first be determined.

2.3 Derivation of the Electron Spin Matter Wave Radius, to Meet the Spin Angular Momentum Quantum Criteria.

The reason for the necessity of this parameter, which is primarily apparent in the first two orbit shells, is explained as follows.

When, via the mechanism proposed in [8], a spinning electron makes a transition into any circular orbital, because there is no spin induction in a circular orbital, the value of angular spin rate carried by the electron will remain unchanged. At the same time if the spin angular momentum does not meet the quantum criteria, the only parameter that can vary in order to meet this is the electron spin matter wave radius, and it is proposed that this parameter thereby increases accordingly towards meeting this criteria.

In any elliptic orbital, exactly the same effect will take place but in addition, due to spin induction, the magnitude of spin angular rate will also increase, both parameters thereby contributing to meeting the spin angular momentum quantum criteria.

Also it will be seen that this effect is not only significant in these orbital energy correction terms, but is also central to the manner in which orbital transitions are initiated. These issues will be further discussed in detail in Section 5.4.

To determine the magnitude of the spin matter wave radius in each orbital, it is necessary to derive a precise expression for the electron spin angular momentum, which can then be equated to the quantum criteria. The resulting expression can then be solved for the spin matter wave radius. This is pursued as follows.

Consider again Fig. 2.1. If the mass surface density of the electron shell is $\Delta m'_e$, then the rest mass of the elemental is

$$\Delta m_e = \Delta m'_e \Gamma_e^2 \sin \theta d\theta d\phi \quad (2.32)$$

The spin velocity of the elemental is

$${}_e v_{sp} = {}_e \omega_{sp} \Gamma_e \sin \theta \quad (2.33)$$

and so the relativistically adjusted mass of the elemental is

$$\Delta m_e^* = \frac{\Delta m'_e \Gamma_e^2 \sin \theta d\theta d\phi}{\left(1 - \frac{{}_e \omega_{sp}^2 \Gamma_e^2 \sin^2 \theta}{c^2}\right)^{1/2}} \quad (2.34)$$

Finally, the relativistically adjusted spin angular momentum of the elemental is then given by

$$\Delta M_e^* = \frac{{}_e \omega_{sp} \Delta m'_e \Gamma_e^4 \sin^3 \theta d\theta d\phi}{\left(1 - \frac{{}_e \omega_{sp}^2 \Gamma_e^2 \sin^2 \theta}{c^2}\right)^{1/2}} \quad (2.35)$$

In evaluating the integral of (2.35), two problems arise, first, the Lamb Shift is, in the low orbit shells, very sensitive to this particular process and it is therefore necessary to obtain as precise a solution as possible. Because the integration of (2.35) over the surface of the electron shell involves a version of the complete elliptic integral of the first kind, its exact evaluation in terms of analytic functions is not possible. Secondly, in order to determine values, it is clearly necessary to know the value of ${}_e \omega_{sp}$ and a method of determining this parameter to the required accuracy and precision is not clear. Consequently, because of these problems, an empirical method of completing the solution must be adopted as follows.

First perform a binomial expansion of (2.35) and write its integration as

$$M_e^* = {}_e \omega_{sp} \Delta m'_e \Gamma_e^4 \int_{\phi=0}^{2\pi} \int_{\theta=0}^{\pi} \left(\sin^3 \theta + \frac{{}_e \omega_{sp}^2 \Gamma_e^2}{2c^2} \sin^5 \theta - \frac{3}8 \frac{{}_e \omega_{sp}^4 \Gamma_e^4}{c^4} \sin^7 \theta + \dots \right) d\theta d\phi \quad (2.36)$$

Perform the first simple integral with respect to ϕ and, taking advantage of symmetry, write the result as

$$M_e^* = 4\pi_e \omega_{sp} \Delta m_e' \Gamma_e^4 \int_{\theta=0}^{\pi/2} \left(\sin^3 \theta + \frac{e \omega_{sp}^2 \Gamma_e^2}{2c^2} \sin^5 \theta - \frac{3}{8} \frac{e \omega_{sp}^4 \Gamma_e^4}{c^4} \sin^7 \theta + \dots \right) d\theta \quad (2.37)$$

Now integrate with respect to θ retaining all terms to give

$$M_e^* = 4\pi_e \omega_{sp} \Delta m_e' \Gamma_e^4 \left(\frac{2}{3} + \frac{4}{15} \frac{e \omega_{sp}^2 \Gamma_e^2}{c^2} - \frac{6}{35} \frac{e \omega_{sp}^4 \Gamma_e^4}{c^2} + \dots \right) \quad (2.38)$$

and this can be written

$$M_e^* = 4\pi_e \omega_{sp} \Delta m_e' \Gamma_e^4 \left(\frac{2}{3} + \sum_{k=2}^{\infty} \frac{(-1)^k 2k}{(2k-1)(2k+1)} \left(\frac{\omega_{sp} \Gamma_e}{c} \right)^{2(k-1)} \right) \quad (2.39)$$

From Appendix B it is seen that when $e \omega_{sp} \Gamma_e \rightarrow c$, the surface area of the spinning electron approaches half that of its rest mass value. Therefore incorporating this and putting $e \omega_{sp} \Gamma_e = k' / c$ in (2.39) gives

$$M_e^* = \frac{4}{3} k' / c \Gamma_e m_e \left(1 + \frac{3}{2} \sum_{k=2}^{\infty} \frac{(-1)^k 2k}{(2k-1)(2k+1)} k'^{/2(k-1)} \right) \quad (2.40)$$

and the restrictions on k' / c such that the solution converges to a positive mean value are that (i) its value must be close to unity and, (ii) it must, when (2.40) is equated to the spin angular momentum quantum criteria, enable a unique solution for Γ_e such that the Lamb Shift, in all orbitals in which it is apparent, is correctly determined.

Thus equating (2.40) to the spin angular momentum quantum criteria and solving for Γ_e gives

$$\Gamma_e = \frac{3_e n_{sp} \hbar}{8\pi k' / c m_e \left(1 + \frac{3}{2} \sum_{k=2}^{\infty} \frac{(-1)^k 2k}{(2k-1)(2k+1)} k'^{/2(k-1)} \right)} \quad (2.41)$$

In (2.41) the summation, with suitable empirical values of k' / c must be taken to sufficient terms such that it has completely converged. This will then provide a value of Γ_e for each orbital for insertion in (2.31). This final evaluation is developed in Section 3.0.

2.4 The Distributed Nature of the Charge on the Nucleus.

To some extent the effect of the nucleus has already been accomplished in that account has been taken of the distance of it from the central point of orbital rotation. However, the nucleus also carries a charge and the question arises as to whether the distributed nature of this charge affects orbital energy in the same manner as that of the electron. There is no doubt that this must be so but because, in the case of hydrogen, the nucleus is so much smaller than the electron, its

charge distribution contribution is not apparent as a fine structure correction. This would not necessarily be the case in other atoms/ions in which the nucleus contained additional protons, as well as neutrons. Consequently, the theoretical relationships developed herein from this point on are strictly only applicable to hydrogen.

3 Determination of the Orbital Energy Correction Terms.

3.1 The Energy Correction Term Due to the Dynamic Distance of the Nucleus from the Central Point of Orbital Rotation.

Extracting this term from (2.31) gives

$$\langle E_{corr,r_p} \rangle = \frac{Ze^2 r_p^2}{4r_e^3} \quad (3.1)$$

In [9], Eq.(3.30) it was shown that

$$\langle r_e \rangle = \frac{L_e}{(1-\varepsilon^2)^{1/2}} = \frac{M_{e,j}^2}{Ze^2 m_e (1-\varepsilon^2)^{1/2}} = \frac{nn_j h^2}{4\pi^2 Ze^2 m_e} \quad (3.2)$$

By similar reasoning concerning the orbit of the nucleus about the central point of rotation, it is proposed that

$$\langle r_p \rangle = \frac{L_p}{(1-\varepsilon^2)^{1/2}} = \frac{M_{p,j}^2}{Ze^2 m_p (1-\varepsilon^2)^{1/2}} = \frac{nn_j h^2}{4\pi^2 Ze^2 m_p} \quad (3.3)$$

So that

$$\frac{\langle r_p^2 \rangle}{\langle r_e^3 \rangle} = \frac{4\pi^2 Ze^2 m_e^3}{nn_j h^2 m_p^2} \quad (3.4)$$

and so in (3.1) this gives

$$\langle E_{corr,r_p} \rangle = \frac{\pi^2 Z^2 e^4 m_e^3}{nn_j h^2 m_p^2} \quad (3.5)$$

and for the purposes of combining with previous results and for numerical computation (3.5) can be re-written

$$\langle E_{corr,r_p} \rangle = \frac{hR_{hy} Z^2 \kappa^2 Z^2}{n^2} \left(\frac{m_e^2}{2\kappa^2 Z m_p^2} \frac{n^3}{n_j} \right) \quad (3.6)$$

3.2 The Energy Correction Term Due to the Distributed Nature of Electron Charge as Augmented by its Spin Matter Wave Radius.

Extracting this term from (2.31) gives

$$\langle E_{corr,\Gamma_e} \rangle = \frac{5Ze^2 \Gamma_e^2}{24r_e^3} \quad (3.7)$$

Insertion of (3.2) gives

$$\langle E_{corr,\Gamma_e} \rangle = \frac{40\pi^6 Z^4 e^8 m_e^3 \Gamma_e^2}{3n^3 n_j^3 h^6} \quad (3.8)$$

and for the purposes of combining with previous results and for numerical computation (3.8) can be re-written

$$\langle E_{corr,\Gamma_e} \rangle = \frac{hR_{hy} Z^2}{n^2} \frac{\kappa^2 Z^2}{n^2} \left(\frac{5\pi^2 m_e^2 c^2 \Gamma_e^2}{3h^2} \frac{n}{n_j^3} \right) \quad (3.9)$$

In (3.9) the numerical value of Γ_e in all orbitals is determined from (2.41) by insertion of appropriate values for $k//$ and taking the summation to 200 terms to ensure convergence. In performing this evaluation it is to be noted that any spherical body possessing mass, if spinning at a high enough angular rate, will be subject to centrifugal force. Unless such a body is infinitely rigid it will consequently distort by expanding normal to the axis of rotation. It is necessary to allow for this condition here and an allowance of $\sim +7.5\%$ has been inserted to cover the centrifugal force expansion of Γ_e due to its high spin rate. This is not in conflict with the Lorentz - Fitzgerald contraction of the circumference because Γ_e is normal to the direction of spin motion.

In the above allowance for centrifugal distortion, and for the general determination of Γ_e , cognisance has been taken of the requirement to optimise the orbital energy intervals so as to ensure that the Lamb Shift in all orbitals was present. This will be discussed in more detail in Sections 5 and 6 below.

The result of this evaluation of Γ_e for all orbitals in the first eight shells are shown in Table 3.1 below.

n	Eccentricity	Electron Matter Wave Radius Γ_e				State
		$e n_{sp} = +0.5$ Orbitals		$e n_{sp} = -0.5$ Orbitals		
8	0	k(+)	1.275E-11		N/A	Γ_e at Point of Transition
8	0.4841	i(+)	3.50E-13	k(-)	3.50E-13	
8	0.6614	h(+)	3.50E-13	i(-)	3.50E-13	
8	0.7806	g(+)	3.50E-13	h(-)	3.50E-13	
8	0.866	f(+)	3.50E-13	g(-)	3.50E-13	
8	0.927	d(+)	3.50E-13	f(-)	3.50E-13	
8	0.9682	p(+)	1.276E-11	d(-)	3.50E-13	
8	0.9922	s	1.325E-11	p(-)	3.50E-13	
7	0	i(+)	1.275E-11		N/A	
7	0.5151	h(+)	3.50E-13	i(-)	3.50E-13	
7	0.6999	g(+)	3.50E-13	h(-)	3.50E-13	
7	0.8207	f(+)	3.50E-13	g(-)	3.50E-13	
7	0.9035	d(+)	3.50E-13	f(-)	3.50E-13	
7	0.9583	p(+)	1.276E-11	d(-)	3.50E-13	
7	0.9897	s	1.325E-11	p(-)	3.50E-13	
6	0	h(+)	1.275E-11		N/A	
6	0.553	g(+)	3.50E-13	h(-)	3.50E-13	
6	0.745	f(+)	3.50E-13	g(-)	3.50E-13	
6	0.866	d(+)	3.50E-13	f(-)	3.50E-13	
6	0.943	p(+)	1.276E-11	d(-)	3.50E-13	
6	0.986	s	1.325E-11	p(-)	3.50E-13	
5	0	g(+)	1.275E-11		N/A	
5	0.6	f(+)	3.50E-13	g(-)	3.50E-13	
5	0.8	d(+)	3.50E-13	f(-)	3.50E-13	
5	0.917	p(+)	1.276E-11	d(-)	3.50E-13	
5	0.98	s	1.325E-11	p(-)	3.50E-13	
4	0	f(+)	1.275E-11		N/A	
4	0.661	d(+)	3.50E-13	f(-)	3.50E-13	
4	0.866	p(+)	1.276E-11	d(-)	3.50E-13	
4	0.968	s	1.325E-11	p(-)	3.50E-13	
3	0	d(+)	1.275E-11		N/A	
3	0.745	p(+)	1.276E-11	d(-)	3.50E-13	
3	0.943	s	1.325E-11	p(-)	3.50E-13	
2	0	p(+)	1.33E-11		N/A	
2	0.866	s	1.37817E-11	p(-)	3.50E-13	s(+) Meta-Stable
1	0	s	1.36E-11		N/A	Stable

Table 3.1 - Γ_e for Electron Orbitals Up to Shell 8.

It is emphasised that other than for orbitals 2s and 1s, these values only apply at the point of

transition. Also, some of the values of Γ_e so determined are considerably greater than the physical radius of a free electron and it is therefore important to remember that these values only apply to the spin matter wave radius of electrons extant within the structure of the hydrogen atom.

The further significance of the values determined for Γ_e in Table 3.1 will also be discussed in Section 5.

4 Addition of the Energy Correction Terms to the Fine Structure Energy Levels.

The á priori relationship for the fine structure energy levels is given by [9], Eq.(3.39) repeated here for convenience

$${}_eE_{or} = -\frac{hR_{hy}Z^2}{n^2} \left[1 + \frac{\kappa^2 Z^2}{n^2} \left\{ \begin{array}{l} \frac{n}{n_\phi^*} - \frac{m_e}{m_0} \left(1 - \frac{\gamma_p m_e}{m_p} \right) \frac{n_e n_{sp}}{n_j n_\phi^*} \\ + 2 \frac{m_e^2}{m_0 m_p} \gamma_p \delta_p \frac{n_e n_{sp} p n_{sp}}{n_\phi^* n_j^2} - \frac{3}{4} \end{array} \right\} \right] \quad (4.1)$$

Adding the orbital energy correction terms, (3.6) and (3.9), to (4.1) provides a new complete relationship for the electron fine structure orbital energy as

$${}_eE_{or} = -\frac{hR_{hy}Z^2}{n^2} \left[1 + \frac{\kappa^2 Z^2}{n^2} \left\{ \begin{array}{l} \frac{n}{n_\phi^*} - \frac{m_e}{m_0} \left(1 - \frac{\gamma_p m_e}{m_p} \right) \frac{n_e n_{sp}}{n_j n_\phi^*} \\ + 2 \frac{m_e^2}{m_0 m_p} \gamma_p \delta_p \frac{n_e n_{sp} p n_{sp}}{n_\phi^* n_j^2} \\ - \frac{m_e^2}{2\kappa^2 m_p^2 Z^2} \frac{n^3}{n_j} - \frac{5\pi^2 m_e^2 c^2 \Gamma_e^2}{3n^2} \frac{n}{n_j^3} - \frac{3}{4} \end{array} \right\} \right] \quad (4.2)$$

This relationship is of course, as previously stated, despite the presence of Z , only applicable in fine detail to hydrogen. It is also subject to the Selection Rules as defined in [8], and to the parametric quantisation of Γ_e as determined in Table 3.1. Subject to these restrictions it is used to produce the energy levels and emission spectra for hydrogen, (vacuum and for $\lambda > 2000\text{\AA}$, air), as presented in Appendix A and which, with all other pertinent results, are discussed in detail below.

5 Discussion of Results.

With the development and addition of the energy correction terms, incorporating the Lamb Shift, in this paper, the resurrection of the Bohr/Sommerfeld theory of atomic structure has reached a state whereby a direct comparison of the achieved results may be made with data published in the literature, in particular, [5]. This reference was, in part, compiled from [12] and in doing so the results have been truncated down to four and three decimal places. Nevertheless, for the purpose of this comparison it is assumed that [5] are the most accurate published data for the electron orbital energy levels and emission spectra for hydrogen.

As stated previously, the development here has, in the interests of brevity and clarity been restricted to hydrogen and it is on the results for that element that the ensuing discussion entirely concentrates.

The results presented in Appendix A should be reviewed in depth to fully appreciate this discussion.

5.1 The Spectral Signature.

The primary results here are those for the emission spectra resulting from transitions from any permitted orbital to the ground state. These spectra, as quoted in [5], are for transitions observed in vacuum and as can be seen from Appendix A, for those orbitals shown, the results are in complete agreement with those in [5]. That this is so not only provides credence to the concept with which the energy correction terms incorporating the Lamb Shift have been developed in this paper but, also to the prior parts of the theory presented in the earlier papers [6] to [9].

When reviewing all other spectra, it is noted that in [5] these are quoted as pertaining to spectra observed in air. Consequently cognisance of the refractive index of air, Π_{air} , has to be taken. To ensure the comparison with [5] was specific to the different theoretical aspects only, Π_{air} as used here was calculated from [12], and is shown in Table A.2.

From the results of this comparison it can be seen that there is excellent agreement between the two sources of data, Appendix A and [5]. Differences range from 0.0001\AA , $\{4d(+) \rightarrow 2p(+)\}$, at 4861\AA , (2.06E-6)%, to 0.2356\AA , $\{8k(+) \rightarrow 7i(+)\}$, at 190567\AA , (1.24E-4)%. This very small level of difference would be due to the very small variances in the values of the constants used in this series of papers, and those in [5] and [12]. Also, in this paper, only a single value of Π_{air} has been calculated for each set of transitions between individual orbit shells. This will introduce a small variation across the orbitals in each shell. Finally, there are very small orbital energy differences which may also contribute. These are discussed below.

5.2 The Energy Levels.

Comparison of orbital energy levels between those in Appendix A and those in [5], show there is a very small difference in all orbit shells ranging from $\sim 0.0320\text{cm}^{-1}$, (3.89E-5)%, in shell 2 to $\sim 0.0496\text{cm}^{-1}$, (4.50E-5)%, in shell 8. Within each shell there is a small variation about these values according to orbital. These differences will in part be due to the slightly different values of the constants used, (see Table A.1). However, the variances are all negative indicating that there is still a small systemic difference between the two theories. This is not considered a very significant point however, because the most important of the atomic structure attributes is the spectra, which can be experimentally measured and thereby compared directly with theory. Nevertheless, it is possible that the small difference in orbital energy above can be further reduced as discussed below in Section 5.6.

5.3 The Lamb Shift.

The Lamb Shift is the $s(+) \rightarrow p(-)$ energy interval for those orbit shells in which this effect is apparent. The short table below shows this interval for the first eight shells as a comparison between [5] and the results in Appendix A.

Shell	s(+) → p(-) Energy Interval, (cm ⁻¹)	
	[5]	Appendix A
2	0.0353	0.0353
3	0.0105	0.0096
4	0.0044	0.0040
5	0.0023	0.0021
6	0.0013	0.0012
7	0.0008	0.0008
8	-	0.0005

Table 5.1 - Lamb Shift Intervals.

The result for the second shell is significant because the value of Γ_e for the 2s(+) orbital was determined in conjunction with the 2p(-) orbital to give exactly the experimental difference value for these orbitals, (0.0352834087 cm⁻¹ or 1057.77Mc/s). The other applicable intervals for shells three to eight in the above table are then predetermined by the need to meet both the spin angular momentum quantum criteria and the conditions determining transition. These are further discussed in Section 5.4 below.

As can be seen from the above table for the applicable orbital energy intervals in shells three to eight there are some very small differences between [5] and the results in Appendix A. These will be due to the same factors discussed above for the orbital energy differences. Improvement may also be effected here via the discussion in Section 5.6.

5.4 The Electron Spin Matter Wave Radius and the Mechanics of Orbital Transition.

The discussion here will be aided by reference to Table 3.1 and Fig. 5.1. The latter shows two plots. The first, (1), is a plot of ${}_e\omega_{sp}$ vs Γ_e for when their product is equal to c , the velocity of light, i.e. this is a plot of ${}_e\omega_{sp}$ vs Γ_e at the point of orbital transition. The second plot, (2), is a plot of ${}_e\omega_{sp}$ vs Γ_e at the point when the electron spin angular momentum quantum criteria is met. The important point about these plots is that they cross, at $\Gamma_e \approx 1.3409\text{E-}11\text{cm}$, ${}_e\omega_{sp} \approx 2.2358\text{E+}21\text{rads/sec.}$, i.e. at point A. It is this that determines which orbitals are "unstable" and result in a transition, and those which are stable, 1s(+), or "meta-stable", 2s(+). The manner in which this is effected is examined in detail below.

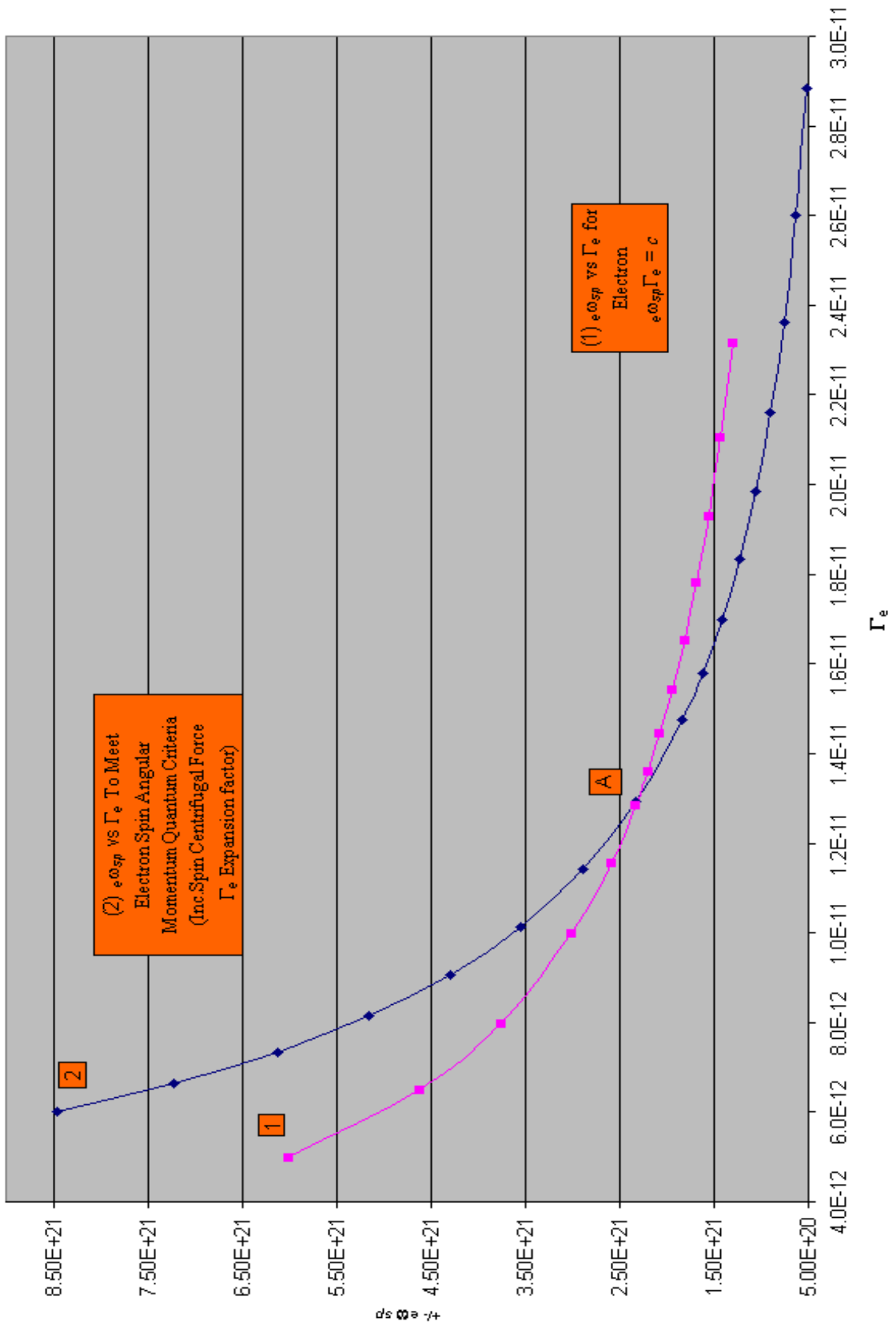


Fig. 5.1.1 - $e \omega_{sp}$ vs Γ_e for (1) $e \omega_{sp} \Gamma_e = c$, and (2) to Meet the Spin Angular Momentum Quantum Criteria.

(i) Consider first the spin-up and spin-down orbitals other than the circular and s orbitals in Table 3.1. When an electron makes a transition into one of these orbitals, (to the left of Lines 1 and 2 in Fig. 5.1), its spin will increase in magnitude, (+ or -), according to which quadrant of the orbital it is in. At the same time its spin matter wave radius, Γ_e will also increase such that their product tends towards providing conformance to the spin angular momentum quantum criteria. Before the latter is accomplished however, the circumferential velocity of the electron reaches the velocity of light, i.e. the product ${}_e\omega_{sp}\Gamma_e$ reaches Line 1, (above point A), in Fig. 5.1, and a further transition occurs.

In the high shell numbers, ($> 3^{rd}$), the spectra are relatively insensitive to the value of Γ_e in the applicable orbitals and therefore the initial value of Γ_e determined for them is 3.50E-13 cm., just above the widely quoted value of $\sim 2.818\text{E-}13$ cm., the physical radius of the free electron. The one exception is the 3p(+) orbital for which an initial value of 1.33E-11cm. has been determined, giving the best fit with [5] for the applicable air spectra.

(ii) Now consider the circular orbitals other than the ground state, 1s orbital. When the electron makes a transition into a circular orbital, it is not subject to spin induction for reasons discussed in [8]. Consequently, the value of ${}_e\omega_{sp}$ possessed by the electron will remain unchanged while it is in these orbitals. Γ_e will therefore simply expand to meet the spin angular momentum quantum criteria. Once again, before that criteria is satisfied the velocity of the electron circumferential surface reaches the velocity of light and a further transition occurs.

The value of Γ_e determined for these circular orbitals is 1.33E-11 cm., for 2p(+) and 1.275E-11 cm. for the rest, which, in conjunction with the value for all other orbitals provides the best fit with [5] for the applicable air spectra.

(iii) Now consider the s orbitals other than 1s and 2s. These orbitals only contain spin-up electrons. When an electron makes a transition into one of these orbitals its spin angular rate and spin matter wave radius will react as for the other elliptic orbitals discussed above and a further transition takes place.

The value of Γ_e determined for these orbitals, 1.325E-11 cm., provides in conjunction with the other orbitals discussed above the best fit for the Lamb Shift for the 3^{rd} to 8^{th} shell. The fact that the spin angular rate is lower and the value of Γ_e higher at transition than in most other elliptic orbitals so far discussed is believed due to the nature of the transition path into these orbitals. This last point also affects the last two orbitals to be discussed, 1s and 2s.

(iv) The 2s orbital. This is the so called "meta-stable" orbital. When an electron makes a transition into 2s, due to the characteristics of the insertion path, its spin, (+ve), will be low enough such that Γ_e can increase to a value that, together with the spin induced increased angular rate, provides conformance to the spin angular momentum quantum criteria. i.e. the product ${}_e\omega_{sp}\Gamma_e$ reaches Line 2, (below point A), in Fig. 5.1. At that instant the electron is stable and can remain so in the 2s orbital until it moves into the next quadrant whereupon its spin reverses and it has made an internal shell transition to the 2p(-) orbital, (same ε and n_j with ${}_en_{sp}$ changing from $+1/2$ to $-1/2$ and n_ϕ^* from $+1/2$ to $+1 1/2$). This phenomenon was presented and described in detail in [8]. Γ_e falls to its 2p(-) value as the electron passes through the dead zone and the spin reverses. The electron can then make a normal 2p(-) \rightarrow 1s ground state transition. This is proposed as the means by which electrons escape from the 2s "meta-stable" orbital. If this mechanism did not exist, in a large volume of hydrogen, there would be two ionisation energies, one for ionisation from 1s, the 13.6eV existing level and one from the 2s orbital which would be $\sim 3.4\text{eV}$.

The value of Γ_e determined for the 2s orbital is that at meta-stability, i.e. 1.37817E-11 cm., which

in conjunction with that in the 2p(-) gives an orbital energy interval equivalent to the 1057.77Mc/s Lamb Shift in shell 2 as mentioned in Section 5.3 above.

(v) Finally, consider the 1s ground state circular orbital. When an electron makes a transition into the ground state, due to the characteristics of the insertion path its spin angular rate will be sufficiently low so that Γ_e can increase to a value that results in their product providing conformance to the spin angular momentum quantum criteria. As the ground state orbital is circular, there is no spin induction and the electron is therefore permanently stable in this orbital.

The value determined for Γ_e , 1.36E-11 cm. is therefore that which gives the appropriate energy correction in this orbital such that the spectral response for transitions directly into the ground state from any permitted orbital is in agreement with [5] for the vacuum spectral lines.

5.5 Ionisation.

Any volume of hydrogen, irradiated at a level in excess of 13.6eV will ionise. To simulate this using the mathematical formulation in the modern quantum mechanics version of atomic structure theory, means raising the principle quantum number, n , to infinity. This in turn means that the electron must be moved to an infinite distance from the proton before it becomes disassociated from it. In reality of course this is not true as in the laboratory ionisation takes place within the physical confines of laboratory equipment.

In the theory presented here, in order to simulate ionisation using (4.2), it is only necessary to raise n to the values shown in the following table.

Orbital Identifier	Orbital at Ionisation	n
1	s(+); p(-)	6,742,908
2	p(+); d(-)	13,485,815
3	d(+); f(-)	20,228,723
4	f(+); g(-)	26,971,630
5	g(+); h(-)	33,714,538
6	h(+); i(-)	40,457,445
7	i(+); k(-)	47,200,353
8	k(+) etc	53,943,260

Table 5.3 - Ionisation Principle Quantum Numbers.

The reason is that all terms in (4.2) decrease in magnitude as n increases, but one term, that for the energy correction term resulting from the dynamic distance of the proton from the central point of orbital rotation, decreases slower than all other terms, (proportional to $1/n$). This term is positive and becomes the dominant term at the above values of n , i.e. the orbital energy has become positive which means that the electron has become disassociated from the proton and the atom has ionised. The above values of n at ionisation follows the orbital eccentricity pattern as is seen by comparing Table 5.3 with [9] Table 3.1. The eccentricities of the above orbitals are however very much closer to unity than in the reference. For instance, the apparent eccentricity in the first entry in Table 5.3 is $(1 - 2.199406639E-14)^{1/2}$. The apparent eccentricity of the orbital in the last entry is $(1 - 2.199406965E-14)^{1/2}$. The calculation of these virtually identical values, [9],

Eq.(3.18), does not however, take into account the very small additional energy terms determined in this paper which provide the difference to make ε exceed unity.

It is appropriate to designate the above ionisation quantum numbers as n_i . It is a matter of interest that the value of n_i for any orbital can be calculated from the following simple formulae.

$$n_i(k) = kn_i(1) - \frac{k}{2} \quad k \text{ even}$$

$$n_i(k) = kn_i(1) - \frac{(k-1)}{2} \quad k \text{ odd}$$

Where,

k is the orbital identifier number in Table 5.3.

Finally, it should be obvious that ionisation cannot take place at any orbital with an eccentricity less than those shown above.

The ionisation energy from the ground state in the resurrected Bohr/Sommerfeld theory presented here is 13.59843288eV.

5.6 Summary.

This summary is to draw together, in simple form, the salient points reviewed above.

(i) The vacuum spectra determined here are in perfect agreement with those in [5], for shells 1 to 8 for all permitted transitions, (in Ångstroms to four decimal places).

Although not reported in Appendix A, spot checks of $np(+)$ to $1s(+)$ spectral emissions were also compared with [5] for shells 10, 20, 30, 40 and 50 again with perfect agreement.

(ii) The air spectra determined here are in agreement to within (1.24E - 4)% worst case with those in [5] for shells 2 to 8 for all permitted transitions, (in Ångstroms to three decimal places).

Although not reported in Appendix A, spot checks of air spectral emissions for a number of random transitions involving very high shell numbers were also compared with [5] with equal or better accuracy to that quoted above.

(iii) The orbital energy levels determined here are in agreement to within typically (4.0E - 5)% with those in [5] for shells 1 to 8, (in cm^{-1} to four decimal places).

(iv) The orbital energy level intervals determined here are in agreement from 0cm^{-1} to 0.0009cm^{-1} for the s to p(-) intervals, shells 2 to 7.

(v) In the dissertation on the mechanics of electron transitions, a means by which electrons "escape" from the meta-stable $2s(+)$ orbital was identified.

(vi) A central factor in the determination of an orbital energy level correction term due to the distributed nature of electron charge, is the variability of the electron spin matter wave radius, a necessity to achieve conformance with the spin angular momentum quantum criteria. This factor is also central to the manner in which orbital transitions are initiated.

(vii) The orbital energy equation has been shown to incorporate the effect of ionisation of the atom and permit the determination of the principle quantum number at ionisation for all orbitals.

5.7 Possible Further Additions/Improvements.

It was stated above that some of the differences between the results achieved here and those in [5] could possibly be further reduced. The means by which that could be effected is threefold as follows.

(i) The Introduction of Magneto-Gyric Effects. - In [9] the derivation of orbital and spin magnetic dipoles assumed that both the electron and the proton nucleus were point source charges. This tacitly assumed that that the so called Magneto-Gyric factors associated with these parameters were unity, (the "2" associated with the spin magnetic dipole was shown to be due to a coupling feature). If cognisance is taken of the fact that the charges on these two particles are uniformly distributed on their surfaces, this will result in their Magneto-Gyric factors being very slightly different from unity. This will in turn make a small adjustment to the orbital energy of the electron which will then result in a similar adjustment to the spectral signature.

(ii) Optimisation of Π_{air} , the Refractive Index of Air. - Although derived with a very high degree of precision, only one value of Π_{air} was used to calculate the air spectra in Table A.3 in the transitions of one orbit shell to another. Account was not taken of the individual transitions from the separate orbitals within each shell. To do so would result in an improvement in the calculated air spectra in Appendix A to those in [5]. To effect this would mean deriving a very precise algorithm that related Π_{air} to spectral wavelength. To ensure sufficient precision, this derivation would have to be based upon Table A.2 and interpolation around each point effected manually.

(iii) Optimisation of Γ_e , the Electron Spin Matter Wave Radius. - The values of Γ_e in (4.2) were only effectively optimised for the first two orbit shells, $n = 1$ and 2, and 3p(+). Precise optimisation for all other orbit shells was not fully explored, partially because it should only be attempted after all systemic features have been incorporated, i.e. as in (i) and (ii) above. Subsequently, it may be possible to further reduce differences in orbital energy and spectral signature between Appendix A and [5] via this parameter.

The exploration of the three above potential improvements to the theory is planned.

6 Conclusions.

The results achieved in this series of papers to resurrect the Bohr/Sommerfeld old quantum theory of atomic structure have been fully discussed and summarised in Section 5 above. These final comments will therefore be restricted to the veracity of the overall development, and its one possibly perceived point of contention, the manner of determination of the electron spin matter wave radius.

This theory is truly not just a resurrection of the old quantum theory of atomic structure, because it recognises and uses throughout the development, the duality of the existence of matter. That combined with the old quantum theory enabled this entire development to be derived from just two basic postulates, those of Planck's quantum energy and de Broglie's matter wave quantum momentum. From the inception of these in [6] through to this paper, the mathematical development, with the exception of the subject discussed below, has been rigorous, with no unsound assumptions, and in which the only approximations taken have been to discard third and higher relativistic terms, that have a negligible impact on the results to the accuracy and precision targeted.

The one exception to the above statement is the manner in which the spin matter wave radius has been determined. In a theory of atomic structure in which the electron is treated as a real physical particle, albeit with a dual corpuscular/wave function existence, and spin is a real param-

eter, it is necessary to know with great precision all of the contributing attributes of that particle. One of the critical requirements in this, and in fact also in the quantum mechanics version, is that the electron conform to the spin angular momentum quantum criteria, howsoever the concept of electron spin is defined. To do that with the electron as treated here, it is first necessary to know accurately and precisely the value of electron spin angular rate. Secondly, bearing in mind the manner in which electron transitions have been defined, the only manner in which the above criteria can be met is, in conjunction with its spin rate, for the electron spin matter wave radius to be a variable. Consequently, it is further necessary to know accurately and with adequate precision the value of this parameter. With the electron as an integral part of an atom, there is no known method with which either of these two parameters can be measured experimentally. Similarly, there is no known way in which they can be determined to the accuracy and precision required purely theoretically, even given the manner of spin inducement proposed in this series of papers. Accordingly, it is therefore necessary to resort to the semi-empirical method of determination adopted here. In doing so it is therefore not unreasonable to tailor the determination process to provide results that match experimentally derived data. This of course is only acceptable, provided that the determination process follows a logical procedure, that integrates smoothly with the rest of the development. It is proposed that this is indeed the case here, as exemplified with particularly the discussion of the initiation of the transition process in Section 5.4 above.

That point accepted, the results obtained here are in excellent agreement with those in the literature. A detailed examination of them, and their numerical calculations, may be obtained from the spreadsheets in which they are computed. See Appendix A.

Finally, any theory of atomic structure does not end with the development to the fine structure level and, in future papers, this theory will be further developed to the level of the hyperfine structure, and to cover the concepts of transition probabilities and spectral intensities, as well as investigation of the potential additions highlighted in the previous Section.

APPENDIX A

Emission Spectra for the First 7 Orbital Shells, (Down to the 3rd), of Hydrogen, (as so far Developed).

This Appendix presents calculated emission/absorption spectra for the first 7 → 3 orbit shells of hydrogen. They include the effects of relativistic mass correction, magnetic dipole coupling and the Lamb Shift. The spectra are calculated using the formula

$$\lambda_{(n)(m)} = \frac{hc}{(E_{or(m)} - E_{or(n)})} \quad (\text{A.1})$$

together with the Selection Rules.

For spectra in which the wavelength is greater than 2000Å, (A.1) is divided by Π_{air} , the refractive index of air, to enable a direct comparison of the results with those in [5].

In (A.1), $E_{or(\#)}$ is given by (4.2) within which n_j is given by [9], Eq.(3.20). R_{hy} is determined from the generalised relationship

$$R_{hy} = \frac{cR_{\infty} \{Zm_p + (J - Z) m_N\}}{\{Zm_p + (J - Z) m_N + m_e\}} \quad (\text{A.2})$$

In this and the other relationships referred to, the values of the parameters used are as shown in the following Table A.1.

Parameter	Name	Value	Units	Ref.
h	Planck's Constant	6.6260693E-27	erg secs	[11]
c	Velocity of Light in Vacuum	2.99792458E+10	cm/sec	[11]
R_{hy}	Rydberg's Constant for Hydrogen	See (A.2)	sec ⁻¹	
R_{∞}	Rydberg's Constant for Infinite Nuclear Mass	1.09737316E+5	cm ⁻¹	[11]
Z	Atomic Number	1 for Hydrogen		
J	Mass Number	1 for Hydrogen		
m_p	Proton Mass	1.67262171E-24	g sec ² /cm	[11]
m_N	Neutron Mass	1.6749278E-24	g sec ² /cm	[11]
m_e	Electron Mass	9.10913826E-28	g sec ² /cm	[11]
e	Electron/Proton Charge	-/+ 4.8032044E-10	esu	See Note 1
γ_p	Proton magnetic moment constant of proportionality	2.79275	-	[2]
δ_p	Proton spin dipole magnetisation constant of proportionality	3.3558912	-	[9]
Π_{air}	Refractive Index of Air	See Table A.2	-	Calculated from [12]

Table A.1 - Parameter Values.

Note 1:- Calculated from $e = 1.60217653E-20$ abcoulombs x c .

Also the following factors have been used to convert energy from ergs to cm⁻¹.

$$\text{Joules} = 1E-7 \text{ ergs}; \quad \text{eV} = 6.24150948E+18 \text{ Joules}; \quad \text{cm}^{-1} = 8.065541E+3 \text{ eV}$$

The values of Π_{air} used, are shown in the following table, as calculated from [12].

Wavelength	Π_{air}
3889	1.000283373820
3970	1.000282912237
4101	1.000282223812
4340	1.000281143049
4861	1.000279342657
6562	1.000276235841
9545	1.000274299185
10049	1.000274132698
10938	1.000273891534
12817	1.000273537699
18751	1.000273036604
19445	1.000273006377
21654	1.000272927044
26251	1.000272823218
37395	1.000272707134
40510	1.000272691823
46525	1.000272669382
74577	1.000272628864
75003	1.000272628349
123682	1.000272605744
190568	1.000272607289

Table A.2 - Π_{air} vs Wavelength.

The only apparent anomaly in this table is that the last two entries appear reversed. This will accentuate any differences to [5] with respect to the emission spectra at the wavelengths concerned.

The calculated orbital energy levels and transition emission spectra are shown below in Table A.3 expressed as wavelengths in Ångstroms.

Orbital Energy - E_{OR}	From		To \rightarrow	n	1			2			3									
	n	n^*_ϕ			0.5	1.5	1.5	0.5	1.5	1.5	0.5	1.5	1.5	0.5	1.5	1.5	0.5	1.5	1.5	
ergs	cm^{-1}	n	n^*_ϕ	n	n^*_ϕ	s(+)	p(+)	s(+)	p(+)	s(+)	p(+)	s(+)	p(+)	s(+)	p(+)	s(+)	p(+)	s(+)	p(+)	
-2.178709E-11	0.0000	1	0.5	s(+)	N.P.															
-5.446796E-12	82258.9163	2	0.5	s(+)	N.P.	N.P.	N.P.	N.P.	N.P.											
-5.446731E-12	82259.2424	2	1.5	p(+)	1215.6683	N.P.	N.P.	N.P.	N.P.											
-5.446803E-12	82258.8810	2	1.5	p(-)	1215.6737	N.P.	N.P.	N.P.	N.P.											
-2.420791E-12	97492.1739	3	0.5	s(+)	N.P.	6.562.9089	6.562.7532	N.P.	N.P.	N.P.	N.P.	N.P.	N.P.	N.P.	N.P.	N.P.	N.P.	N.P.	N.P.	N.P.
-2.420772E-12	97492.2699	3	1.5	p(+)	1025.7219	6.562.7270	N.P.	N.P.	N.P.	N.P.	N.P.	N.P.	N.P.	N.P.	N.P.	N.P.	N.P.	N.P.	N.P.	N.P.
-2.420793E-12	97492.1643	3	1.5	p(-)	1025.7230	6.562.7725	N.P.	N.P.	N.P.	N.P.	N.P.	N.P.	N.P.	N.P.	N.P.	N.P.	N.P.	N.P.	N.P.	N.P.
-2.420765E-12	97492.3035	3	2.5	d(+)	N.P.	N.P.	6.562.8530	N.P.	N.P.	N.P.	N.P.	N.P.	N.P.	N.P.	N.P.	N.P.	N.P.	N.P.	N.P.	N.P.
-2.420772E-12	97492.2692	3	2.5	d(-)	N.P.	N.P.	6.562.8678	6.562.7121	N.P.	N.P.	N.P.	N.P.	N.P.	N.P.	N.P.	N.P.	N.P.	N.P.	N.P.	N.P.
-1.361692E-12	102823.802	4	0.5	s(+)	N.P.	N.P.	4.861.3747	4.861.2893	N.P.	N.P.	N.P.	N.P.	N.P.	N.P.	N.P.	N.P.	N.P.	N.P.	N.P.	N.P.
-1.361684E-12	102823.841	4	1.5	p(+)	972.5367	4.861.2883	N.P.	N.P.	N.P.	N.P.	N.P.	N.P.	N.P.	N.P.	N.P.	N.P.	N.P.	N.P.	N.P.	N.P.
-1.361692E-12	102823.798	4	1.5	p(-)	972.5371	4.861.2986	N.P.	N.P.	N.P.	N.P.	N.P.	N.P.	N.P.	N.P.	N.P.	N.P.	N.P.	N.P.	N.P.	N.P.
-1.361681E-12	102823.855	4	2.5	d(+)	N.P.	N.P.	4.861.3621	N.P.	N.P.	N.P.	N.P.	N.P.	N.P.	N.P.	N.P.	N.P.	N.P.	N.P.	N.P.	N.P.
-1.361684E-12	102823.841	4	2.5	d(-)	N.P.	N.P.	4.861.3654	4.861.2800	N.P.	N.P.	N.P.	N.P.	N.P.	N.P.	N.P.	N.P.	N.P.	N.P.	N.P.	N.P.
-1.361680E-12	102823.862	4	3.5	f(+)	N.P.	N.P.	N.P.	N.P.	N.P.	N.P.	N.P.	N.P.	N.P.	N.P.	N.P.	N.P.	N.P.	N.P.	N.P.	N.P.
-1.361681E-12	102823.855	4	3.5	f(-)	N.P.	N.P.	N.P.	N.P.	N.P.	N.P.	N.P.	N.P.	N.P.	N.P.	N.P.	N.P.	N.P.	N.P.	N.P.	N.P.
-8.714811E-13	105291.578	5	0.5	s(+)	N.P.	N.P.	4.340.4998	4.340.4317	N.P.	N.P.	N.P.	N.P.	N.P.	N.P.	N.P.	N.P.	N.P.	N.P.	N.P.	N.P.
-8.714772E-13	105291.598	5	1.5	p(+)	949.7430	4.340.4347	N.P.	N.P.	N.P.	N.P.	N.P.	N.P.	N.P.	N.P.	N.P.	N.P.	N.P.	N.P.	N.P.	N.P.
-8.714815E-13	105291.576	5	1.5	p(-)	949.7482	4.340.4388	N.P.	N.P.	N.P.	N.P.	N.P.	N.P.	N.P.	N.P.	N.P.	N.P.	N.P.	N.P.	N.P.	N.P.
-8.714768E-13	105291.605	5	2.5	d(+)	N.P.	N.P.	4.340.4948	N.P.	N.P.	N.P.	N.P.	N.P.	N.P.	N.P.	N.P.	N.P.	N.P.	N.P.	N.P.	N.P.
-8.714772E-13	105291.598	5	2.5	d(-)	N.P.	N.P.	4.340.4962	4.340.4281	N.P.	N.P.	N.P.	N.P.	N.P.	N.P.	N.P.	N.P.	N.P.	N.P.	N.P.	N.P.
-8.714751E-13	105291.608	5	3.5	f(+)	N.P.	N.P.	N.P.	N.P.	N.P.	N.P.	N.P.	N.P.	N.P.	N.P.	N.P.	N.P.	N.P.	N.P.	N.P.	N.P.
-8.714768E-13	105291.605	5	3.5	f(-)	N.P.	N.P.	N.P.	N.P.	N.P.	N.P.	N.P.	N.P.	N.P.	N.P.	N.P.	N.P.	N.P.	N.P.	N.P.	N.P.
-8.714747E-13	105291.610	5	4.5	g(+)	N.P.	N.P.	N.P.	N.P.	N.P.	N.P.	N.P.	N.P.	N.P.	N.P.	N.P.	N.P.	N.P.	N.P.	N.P.	N.P.
-8.714751E-13	105291.608	5	4.5	g(-)	N.P.	N.P.	N.P.	N.P.	N.P.	N.P.	N.P.	N.P.	N.P.	N.P.	N.P.	N.P.	N.P.	N.P.	N.P.	N.P.

Continued on next page.

Table A.3 - Line Spectra for the First Seven to Three Orbital Shells of Hydrogen

The spreadsheet that produced Table A.3 covers a wider orbit shell range and is available for download as:-

HydrogenSpectra.xls.

This spreadsheet is cell locked but contains a small area highlighted at the bottom of the 1st sheet wherein a spot check of any desired transition can be performed via the input of just six parameters in six unlocked cells. Ionisation levels can also be checked here.

Two other sheets are incorporated in this spreadsheet

- (i) the relevant orbital energy levels and spectral wavelengths from [5], and
- (ii) the differences in the values in (i) and the top sheet.

Note that this spreadsheet is a working document that has "evolved" as the development in this series of papers proceeded. Presentation has not therefore been aesthetically optimised.

APPENDIX B.

Surface Area of a Sphere Spinning Such That its

Circumferential Velocity is Equal to the Velocity of Light.

Repeating (2.4)

$$\Delta\Lambda^* = \Gamma_e^2 \sin\theta \cos\theta d\theta d\phi \quad (\text{B.1})$$

Integrating, first with respect to ϕ yields

$$\Lambda^* = 4\pi\Gamma_e^2 \int_0^{\pi/2} \sin\theta \cos\theta d\theta \quad (\text{B.2})$$

where advantage of symmetry with regard to θ has been incorporated.

Evaluation of (B.2) is simple and gives

$$\Lambda^* = 2\pi\Gamma_e^2 \quad (\text{B.3})$$

This is exactly half the surface area of the sphere when at rest, the reduction being caused by the Lorentz - Fitzgerald contraction of circumferential dimensions.

APPENDIX C.

Derivation of the Lorentz - Fitzgerald Contracted Dimensions l_5 and l_6 in Section 2.1.

Consider Fig. C.1 below. This is a plan view of a cross-section of Fig. 2.1 taken at the plane of the elemental.

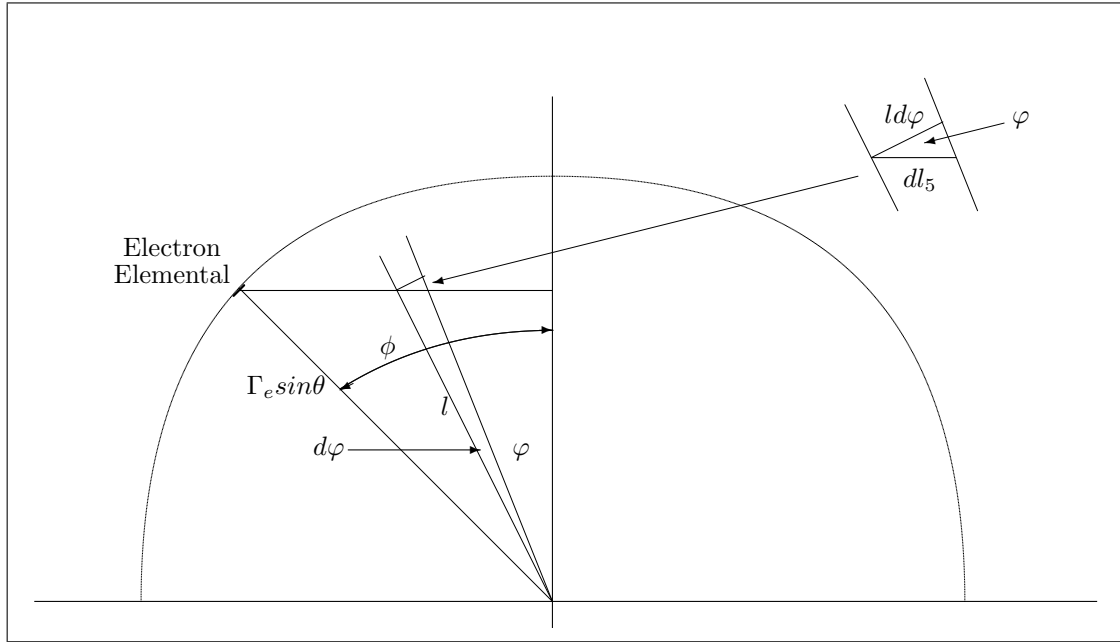


Fig. C.1 - Plan View at Electron Elemental.

From the Figure

$$l = \Gamma_e \sin \theta \cos \phi \sec \varphi \quad (\text{C.1})$$

So that

$$l d\varphi = \Gamma_e \sin \theta \cos \phi \sec \varphi d\varphi \quad (\text{C.2})$$

and therefore the Lorentz - Fitzgerald contracted element of l_5 is given by

$$dl_5 = \Gamma_e \sin \theta \cos \phi \sec^2 \varphi \left(1 - \frac{e\omega_{sp}^2 l^2}{c^2} \right)^{1/2} d\varphi \quad (\text{C.3})$$

Because, by far, the greater part of the contraction takes place at the perimeter, this process can be greatly simplified by the approximation

$$dl_5 = \Gamma_e \sin \theta \cos \phi \sec^2 \varphi \left(1 - \frac{e\omega_{sp}^2 \Gamma_e^2 \sin^2 \theta}{c^2} \right)^{1/2} d\varphi \quad (\text{C.4})$$

The small error that this approximation introduces will be compensated out by way of the process that determines the value of Γ_e .

When $e\omega_{sp}\Gamma_e = c$, (C.4) becomes

$$dl_5 = \Gamma_e \sin \theta \cos \theta \cos \phi \sec^2 \varphi d\varphi \quad (\text{C.5})$$

Integrating

$$l_5 = \Gamma_e \sin \theta \cos \theta \cos \phi \int_0^\phi \sec^2 \varphi d\varphi \quad (\text{C.6})$$

which evaluates to

$$l_5 = \Gamma_e \sin \theta \cos \theta \sin \phi \quad (\text{C.7})$$

Consequently, in Fig. 2.1,

$$l_6 = l_5 \cot \phi = \Gamma_e \sin \theta \cos \theta \cos \phi \quad (\text{C.8})$$

REFERENCES.

- [1] P.A.Cox, *Introduction to Quantum Theory and Atomic Structure*, Oxford Science Publications, 1996 - 2002.
- [2] G.K.Woodgate, *Elementary Atomic Structure*, M^cGraw Hill, 1970.
- [3] E.U.Condon and Hugh Odishaw, *Handbook of Physics*, M^cGraw Hill, 1967.
- [4] Richard P.Feynman, *Quantum Electrodynamics*, Addison Wesley, 1998.
- [5] Charlotte E.Moore, (Edited by Jean W.Gallagher), *Tables of Spectra of Hydrogen, Carbon, Nitrogen and Oxygen Atoms and Ions*, CRC Press, 1993.
- [6] P.G.Bass, *An Investigation of de Broglie Matter Waves in the Relativistic Domain D₀*, www.relativitydomains.com.
- [7] P.G.Bass, *Resurrection of the Bohr/Sommerfeld Theory of Atomic Structure - [1] - Basic Orbits Including Relativistic Mass Increase Effects*, www.relativitydomains.com.
- [8] P.G.Bass, *Resurrection of the Bohr/Sommerfeld Theory of Atomic Structure - [2] - Incorporation of the Mechanical Effects of Electron Spin*, www.relativitydomains.com.
- [9] P.G.Bass, *Resurrection of the Bohr/Sommerfeld Theory of Atomic Structure - [3] - Magnetic Dipole Coupling*, www.relativitydomains.com.
- [10] P.G.Bass, *The Special Theory of Relativity - A Classical Approach*, Apeiron (4) Vol.10 October 2003, (Also on www.relativitydomains.com).
- [11] The National Institute of Science and Technology, (NIST), *On Line Constants Database*, www.NIST.com
- [12] J.D.Garcia and J.E.Mack, *Energy Levels and Line Tables for One Electron Atomic Spectra*, Journal of the Optical Society of America, Vol.55 No.6 pg. 654 - 685.